Available online at www.sciencedirect.com
SCIENCE DIRECT®
Journal of Sound and Vibration 280 (2005) 883–902
JOURNAL OF SOUND AND VIBRATION
www.elsevier.com/locate/jsvi

Exact substructuring in recursive Newton's method for solving transcendental eigenproblems

M.S. Djoudi[a], D. Kennedy[a,*], F.W. Williams[b], S. Yuan[c], K. Ye[c]

[a]*Cardiff School of Engineering, Cardiff University, P.O. Box 925, The Parade, Cardiff CF24 0YF, UK*
[b]*Department of Building and Construction, City University of Hong Kong, Tat Chee Avenue, Kowloon, Hong Kong*
[c]*Department of Civil Engineering, Tsinghua University, Beijing 100084, P.R. China*

Received 10 July 2003; accepted 18 December 2003

Abstract

The well-established Wittrick–Williams (W–W) algorithm guarantees accurate convergence on natural frequencies or critical buckling loads of structures in the transcendental eigenproblems arising from the use of exact member stiffnesses, i.e. dynamic member stiffnesses for vibration. The associated mode calculations had no such guarantee until they were recently greatly improved by solving the transcendental eigenproblem exactly, by reducing it to a generalised linear eigenproblem which is solved by a guided recursive Newton method involving inverse iteration. The present paper demonstrates the benefits of using frequency squared, rather than frequency, as the eigenparameter. Next, exact substructuring is introduced into the recursive Newton method, with accuracy retained because the inverse iteration includes the substructure nodes. If member fixed end eigenvalues lie close to the sought eigenvalue they can cause inaccuracy, or even wrong results, and so they are removed efficiently by inserting interior nodes to create simple substructures. Numerical results for a moderately large structure show that exact substructuring reduces the transcendental eigensolution time without reducing accuracy. Simpler examples designed to be numerically ill conditioned in the absence of interior nodes show that such ill conditioning is almost removed by inserting interior nodes within substructures. Exact substructuring is also applicable to other inverse iteration and W–W algorithm-based methods.

*Corresponding author. Tel.: +44-29-2087-5340; fax: +44-29-2087-4939.
E-mail address: kennedyd@cf.ac.uk (D. Kennedy).

0022-460X/$ - see front matter © 2004 Elsevier Ltd. All rights reserved.
doi:10.1016/j.jsv.2003.12.050

1. Introduction

The Wittrick–Williams (W–W) algorithm [1–3] is a reliable and efficient tool to obtain eigenvalues (natural frequencies in free vibration problems or critical load factors in buckling problems) of transcendental eigenproblems to any required accuracy, in contrast to alternative methods which can miss eigenvalues. The algorithm does not directly compute the eigenvalues, but instead simply finds J, the total number of eigenvalues below an arbitrarily given trial value. In this way upper and lower bounds are established on each required eigenvalue, after which various iterative procedures can be used to converge on the eigenvalue to the required accuracy. An important feature of the algorithm has always been that it permits substructuring [1–3], including powerful multi-level substructuring [4,5]. However a recent advancement uses the W–W algorithm extremely efficiently, because it is analogous to inverse iteration for the linear eigenproblem. The present paper gives a substructuring strategy which is compatible with this recent method. However, earlier work is surveyed first.

One well-known convergence method is the bisection method, which has the advantage that it converges with certainty to any specified accuracy in a predictable number of iterations, but has the disadvantage that it is time consuming when high accuracy is required. Williams and Kennedy [6] developed the multiple determinant parabolic interpolation method which retained the certainty and was shown to offer substantial time savings over bisection for non-coincident eigenvalues. Later the work was extended to efficiently deal also with clusters of close or coincident eigenvalues [7]. Further research on the transcendental eigenvalue problem has recently led to the development of a new member property called the member stiffness determinant [8,9], which can be used to remove the poles in the plot of the determinant of the transcendental overall stiffness matrix against the eigenparameter, leading to simpler and faster eigenvalue location.

Thus the calculation of the eigenvalues for the transcendental eigenproblem has benefited greatly from the W–W algorithm, because it enabled the development of many logical procedures that guarantee convergence on all required eigenvalues with certainty and to any desired accuracy. In contrast, the calculation of the corresponding eigenvectors (i.e. modes) lacked such precision and elegance. The random force method of Hopper and Williams [10] is simple, fast and cheap and so has often been used. However, its mode calculations are much (e.g. 2 significant figures) less accurate than the eigenvalue calculations and the method fails (or is of low accuracy) when the required eigenvalue of a structure coincides with (or is close to) a fixed end eigenvalue of one of its members.

To improve the random force method, Ronagh et al. [11] introduced the interior nodes strategy. This involves inserting interior nodes into members whose fixed end eigenvalues are close to or coincident with the structure eigenvalue and therefore it expands the transcendental stiffness matrix of the structure. This removes the possibility of failure or acute inaccuracy due to coincidence or close proximity of structure and fixed end member eigenvalues, but the modes obtained remain much less accurate than the eigenvalues.

Yuan et al. [12–14] have developed several improved mode calculation methods. The best of these are a new second-order method [13] and its recursive extension [14]. The second-order method uses the circular frequency of vibration, ω, as the eigenparameter in standard inverse iteration, with approximate natural frequencies and the interior node strategy to obtain the

corresponding vibration modes reliably to second-order accuracy. Because this also enables a second-order accuracy natural frequency to be estimated, it led naturally to the recursive method [14], which simultaneously converges to high accuracy on both the required natural frequency and its associated mode. This involves reducing the transcendental eigenproblem to a generalised linear eigenproblem, which is solved with second-order convergence by a guided recursive Newton method involving inverse iteration. Note that the interior node strategy is a substantial advance on earlier [15,16] inverse iteration and Newton-based transcendental eigensolution methods, because it removes an important source of potential ill conditioning.

The present paper primarily extends the recursive Newton method to include exact substructuring, one important application of which is to handle nodes inserted into members as a consequence of the interior node strategy described above. The methods presented are applicable to the many other disciplines in which the W–W algorithm is used (e.g. fluid vibrating in pipes [17], heat and mass diffusion [18,19] and Sturm–Liouville-type mathematical problems [20]), and to buckling [3] as well as vibration problems in structural analysis. However for convenience, but without loss of generality, the theory and applications given in this paper are presented in the context of the free vibration of structures.

In order to present the new contribution of this paper it is necessary to first summarise in concise and suitable form (in Sections 2–4, respectively) the W–W algorithm, exact substructuring and the recursive Newton method. Section 5 then proves for the first time, and illustrates by examples, that the inverse iteration used in the recursive Newton method converges faster if ω^2, rather than ω, is used as the eignenparameter. Therefore Section 6 details the new substructuring method in the context of ω^2, while Section 7 presents the results that this method gives for a demanding choice of numerical examples.

2. The W–W algorithm

When using exact methods for undamped free vibration of structures, solution of the governing differential equations results in the transcendental eigenvalue problem [1]

$$\mathbf{K}(\omega)\mathbf{D} = \mathbf{0}, \tag{1}$$

where $\mathbf{D}$ is the displacement amplitude vector and $\mathbf{K}$ is the transcendental dynamic stiffness matrix, the coefficients of which include trigonometric and hyperbolic functions involving ω and the lengths, rigidities and distributed masses of the members.

This is a more demanding problem than the generalised linear eigenvalue problem of the traditional finite element method (FEM), for which many well-established solution methods are available [21] and whose reliability can be guaranteed using the Sturm sequence property [22]. Such methods cannot be applied directly to the transcendental eigenproblem of Eq. (1), e.g. because natural frequencies may coincide with poles of $|\mathbf{K}(\omega)|$, i.e. values of ω at which $|\mathbf{K}(\omega)| \to \infty$ [2,23]. These methods may also have difficulty in detecting natural frequencies of high multiplicity.

To overcome such difficulties, the natural frequencies of the transcendental eigenvalue problem are found with certainty by applying the W–W algorithm [1], which gives J, the number of natural

frequencies below ω_t, a trial value of ω, as

$$J(\omega_t) = J_0(\omega_t) + s\{\mathbf{K}(\omega_t)\}. \tag{2}$$

Here

$$J_0(\omega_t) = \sum_m J_m(\omega_t), \tag{3}$$

where the summation is over all members of the structure and $J_m(\omega_t)$ is the number of natural frequencies of member m that are exceeded by ω_t if its ends are assumed to be fixed. J_m can be calculated from simple formulae for most commonly used members, or otherwise numerical procedures are available for its calculation [4]. Finally, $s\{\mathbf{K}(\omega_t)\}$ is known as the 'sign count' of $\mathbf{K}(\omega_t)$ and can be calculated as the number of negative leading diagonal elements of $\mathbf{K}^{\Delta}(\omega_t)$, the upper triangular matrix obtained from $\mathbf{K}(\omega_t)$ by the usual form of Gauss elimination, without row interchanges, scaling or pivoting.

Clearly ω_t is a lower bound ω_ℓ on the rth natural frequency ω_r if $J(\omega_t) < r$, and otherwise is an upper bound ω_u. Hence the numbers of natural frequencies N_r and member fixed end natural frequencies N_{r0} lying in the interval (ω_ℓ, ω_u) are given by

$$N_r = J(\omega_u) - J(\omega_\ell), \quad N_{r0} = J_0(\omega_u) - J_0(\omega_\ell). \tag{4}$$

3. Exact substructuring

The W–W algorithm of Eq. (2) is readily extended [5], without approximation, to a problem comprising n_s substructures $S_1, S_2, \ldots, S_{n_s}$ which are each attached to a parent structure S_p at a number of discrete connection nodes. It is well known from its static equivalent, that although substructures are dealt with one by one in order to save computer storage and computation, the whole process can be represented by writing the transcendental eigenproblem of Eq. (1) as

$$\begin{bmatrix} \mathbf{K}_{ii1} & \mathbf{0} & \cdots & \mathbf{0} & \tilde{\mathbf{K}}_{ic1} \\ \mathbf{0} & \mathbf{K}_{ii2} & \cdots & \mathbf{0} & \tilde{\mathbf{K}}_{ic2} \\ \vdots & \vdots & \ddots & \vdots & \vdots \\ \mathbf{0} & \mathbf{0} & \cdots & \mathbf{K}_{iin_s} & \tilde{\mathbf{K}}_{icn_s} \\ \tilde{\mathbf{K}}_{ic1}^{\mathrm{T}} & \tilde{\mathbf{K}}_{ic2}^{\mathrm{T}} & \cdots & \tilde{\mathbf{K}}_{icn_s}^{\mathrm{T}} & \mathbf{K}_{pT} \end{bmatrix} \begin{bmatrix} \mathbf{D}_{i1} \\ \mathbf{D}_{i2} \\ \vdots \\ \mathbf{D}_{in_s} \\ \mathbf{D}_p \end{bmatrix} = \begin{bmatrix} \mathbf{X}_{i1} \\ \mathbf{X}_{i2} \\ \vdots \\ \mathbf{X}_{in_s} \\ \mathbf{X}_p \end{bmatrix}, \tag{5}$$

where

$$\mathbf{K}_{pT} = \mathbf{K}_p + \sum_{s=1}^{n_s} \tilde{\mathbf{K}}_{ccs}. \tag{6}$$

Here the right hand side of Eq. (5) is any vector of forces, which would be null at an eigenvalue, but are shown here to help with the theory of Section 6; the subscripts i and c denote, respectively, for substructure $S_s (s = 1, 2, \ldots, n_s)$ internal degrees of freedom and degrees of freedom which are connected to those of the parent structure; subscript p denotes the parent structure; superscript T denotes the transpose of a matrix; and $\tilde{}$ above matrices indicates the addition of null rows and/or

columns to denote the placement of substructure stiffness contributions at the connection nodes of the parent structure. (Note that the null rows and columns indicated by ˜ are needed for ease of explanation but that coding would not normally introduce them, instead working only with the non-zero coefficients of these matrices.)

Applying Gauss elimination to Eq. (5), but arresting it just before the rows containing $\mathbf{D}_p$ are pivotal gives

$$\begin{bmatrix} \mathbf{K}^{\Delta}_{ii1} & \mathbf{0} & \cdots & \mathbf{0} & \tilde{\mathbf{K}}^{*}_{ic1} \\ \mathbf{0} & \mathbf{K}^{\Delta}_{ii2} & \cdots & \underline{\mathbf{0}} & \tilde{\mathbf{K}}^{*}_{ic2} \\ \vdots & \vdots & \ddots & \vdots & \vdots \\ \mathbf{0} & \mathbf{0} & \cdots & \mathbf{K}^{\Delta}_{iin_s} & \tilde{\mathbf{K}}^{*}_{icn_s} \\ \mathbf{0} & \mathbf{0} & \cdots & \mathbf{0} & \mathbf{K}^{*}_{pT} \end{bmatrix} \begin{bmatrix} \mathbf{D}_{i1} \\ \mathbf{D}_{i2} \\ \vdots \\ \mathbf{D}_{in_s} \\ \mathbf{D}_p \end{bmatrix} = \begin{bmatrix} \mathbf{X}^{*}_{i1} \\ \mathbf{X}^{*}_{i2} \\ \vdots \\ \mathbf{X}^{*}_{in_s} \\ \mathbf{X}^{*}_{p} \end{bmatrix}, \tag{7}$$

where

$$\mathbf{K}^{*}_{pT} = \mathbf{K}_{pT} - \sum_{s=1}^{n_s} \tilde{\mathbf{K}}^{\mathrm{T}}_{ics} \mathbf{K}^{-1}_{iis} \tilde{\mathbf{K}}_{ics}, \tag{8}$$

$\mathbf{K}^{\Delta}_{iis}$ is the upper triangular form of $\mathbf{K}_{iis}$, while $\tilde{\mathbf{K}}^{*}_{ics}$, $\mathbf{X}^{*}_{is}$ and $\mathbf{X}^{*}_{p}$ are modified forms of $\mathbf{K}_{ics}$, $\mathbf{X}_{is}$ and $\mathbf{X}_p$, respectively.

Hence Eqs. (2) and (3) are replaced by

$$J = J_0 + s\left\{\mathbf{K}^{*}_{pT}\right\}, \tag{9}$$

$$J_0 = \sum_{s=1}^{n_s} \left(s\{\mathbf{K}_{iis}\} + \sum_{m \in s_s} J_m \right) + \sum_{m \in s_p} J_m. \tag{10}$$

4. Recursive Newton method in the absence of substructures

Suppose a frequency interval (ω_ℓ, ω_u) has been identified, for example by bisection, which contains one natural frequency ω_g (i.e. $N_r = 1$) and no member fixed end frequencies (i.e. $N_{r0} = 0$). Let ω_a denote the best available approximation to ω_g in (ω_ℓ, ω_u). (Initially ω_a is set to the mid-point of (ω_ℓ, ω_u) to ensure that ω_g is the closest natural frequency to ω_a.) Then better approximations to ω_g and the mode vector $\mathbf{D}_g$ are found by solving the generalised linear eigenvalue problem

$$\mathbf{K}_a \mathbf{D} = \mu[\mathbf{K}'_a \mathbf{D}], \tag{11}$$

where

$$\mathbf{K}_a = \mathbf{K}(\omega_a), \quad \mathbf{K}'_a = \frac{\mathrm{d}\mathbf{K}_a}{\mathrm{d}\omega}, \tag{12}$$

and estimating the eigenvalue ω_g by

$$\omega_\mu = \omega_a - \mu. \tag{13}$$

The force vector $[\mathbf{K}'_a\mathbf{D}]$ is assembled by summing contributions from each member of the structure so that there is no need to form $\mathbf{K}'_a$ explicitly. The necessary derivatives of the element stiffness matrices are obtained fairly easily, either in closed form [14], or by differencing [13], with the former used to obtain the results given in this paper.

Eq. (11) is a typical formulation of Newton's method, and is solved by convergence on ω_g using the inverse iteration procedure

$$\bar{\mathbf{D}}^{(k+1)} = \mathbf{K}_a^{-1}\left[\mathbf{K}'_a\mathbf{D}^{(k)}\right], \tag{14}$$

where superscripts (k) denote values at iteration k and the iterative procedure starts with $\mathbf{D}^{(0)}$ as a random vector. $\bar{\mathbf{D}}^{(k+1)}$ is normalised to give $\mathbf{D}^{(k+1)}$, whose numerically largest element is unity. $\mu^{(k+1)}$ is given by the Rayleigh quotient

$$\mu^{(k+1)} = \frac{\left(\bar{\mathbf{D}}^{(k+1)}\right)^{\mathrm{T}}\left[\mathbf{K}'_a\mathbf{D}^{(k)}\right]}{\left[\bar{\mathbf{D}}^{(k+1)}\right]^{\mathrm{T}}\left[\mathbf{K}'_a\,\bar{\mathbf{D}}^{(k+1)}\right]}. \tag{15}$$

Convergence is terminated when

$$|\mu^{(k+1)} - \mu^{(k)}| < \varepsilon \tag{16}$$

for some pre-defined tolerance ε. The final step of the Newton method uses an alternative expression [14] for $\mu^{(k+1)}$ to improve convergence on $\mathbf{D}_g$.

In Refs. [11–14], interior nodes were automatically inserted in members during the solution process whenever they were required to remove poles of $|\mathbf{K}(\omega)|$. Such poles correspond to fixed end natural frequencies of individual members, i.e. to trial values of ω_t where J_m increases, and hence so does J_0, in Eq. (3). Alternative strategies for where to place the interior nodes have already been presented [13,14]. Interior nodes only need to be inserted temporarily for convergence on particular natural frequencies lying close to the fixed end natural frequencies of individual members. However, for convenience in obtaining the results presented in this paper, any necessary interior nodes have been pre-defined and used during convergence on all the required natural frequencies, and also during the initial separation of the eigenvalues.

Fig. 1 illustrates that, by numbering the interior nodes before the original nodes of the structure, any member containing interior nodes may be regarded as a simple substructure, with no change to the node numbering of its parent structure.

5. Use of ω^2 as the eigenparameter

In the recursive Newton method of Section 4, the eigenvalues are the natural frequencies ω_g of the structure. This approach seems natural from a physical viewpoint. In contrast, the usual FEM

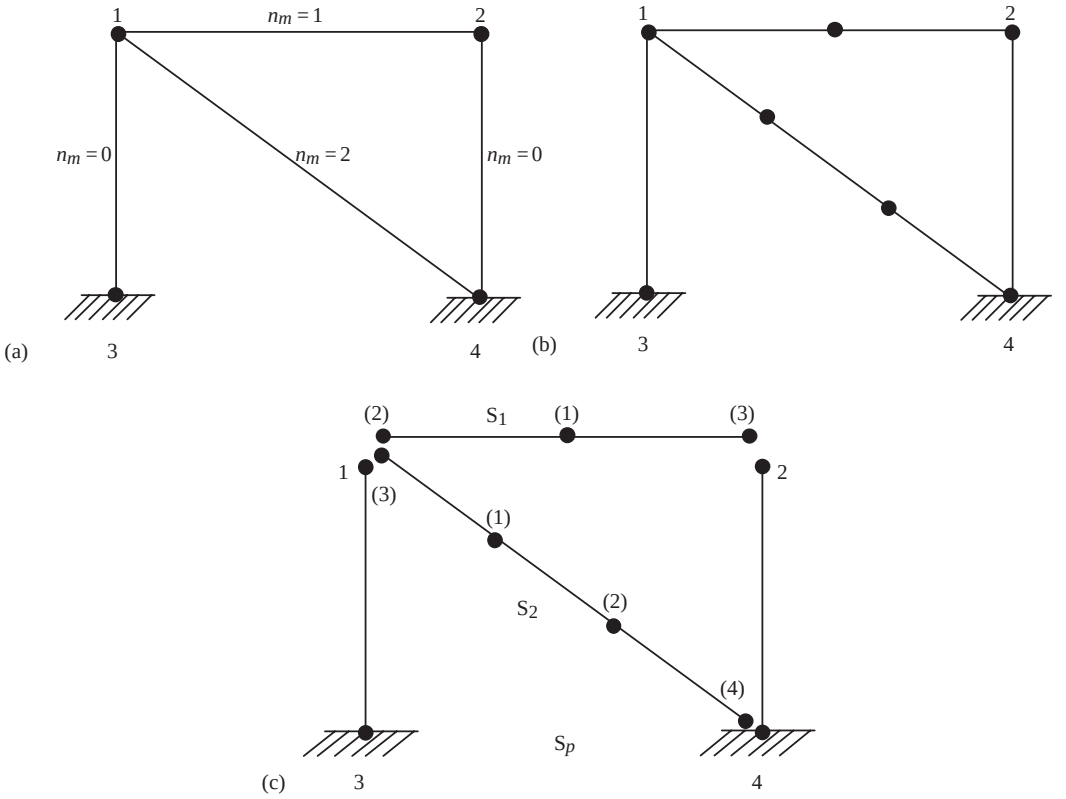

Fig. 1. Interior node substructuring: (a) original frame, with four nodes, showing the number of interior nodes (n_m) to be inserted in each member; (b) addition of interior nodes; (c) parent structure S_p and substructures S_1 and S_2, with node numbers shown in brackets.

gives the linear eigenvalue problem

$$(\mathbf{K} - \Lambda\mathbf{M})\mathbf{D} = \mathbf{0}, \tag{17}$$

where $\Lambda = \omega^2$ and the static stiffness matrix $\mathbf{K}$, the mass matrix $\mathbf{M}$ and the displacement amplitude vector $\mathbf{D}$ relate to a finite number (N) of degrees of freedom at nodes of the structure. Here the eigenparameter is clearly $\Lambda(= \omega^2)$ rather than ω.

In the transcendental eigenvalue problem of Eq. (1), the dynamic stiffness matrix $\mathbf{K}(\omega)$ has often been recognised [15,24] as being identical to the matrix that would be obtained by starting with a hypothetical infinite-order FEM formulation (i.e. letting $N \to \infty$ in Eq. (17)), and using arrested Gauss elimination to eliminate all nodes internal to members. This simple identity must be true, because both matrices relate the same sets of displacement and force amplitudes for any choice of the displacements. Hence it may be better to think in terms of the transcendental stiffness matrix as $\mathbf{K}(\Lambda)$ rather than $\mathbf{K}(\omega)$, i.e. to treat it as a function of ω^2 rather than ω.

This hypothesis is supported by a closer study of the elements of $\mathbf{K}(\omega)$ (e.g. for Bernoulli–Euler [8] and Timoshenko [9] members), when all the trigonometric and hyperbolic functions are

replaced by their expansions. It is seen that every element has an expansion containing only even powers of ω, and so can be regarded as a function of ω^2.

An alternative, $\mathbf{K}(\Lambda)$, formulation of the generalised linear eigenvalue problem of Eqs. (11) and (12) is therefore given by

$$\mathbf{K}_a\mathbf{D} = \mu^*[\mathbf{M}_a\mathbf{D}], \tag{18}$$

where

$$\mathbf{K}_a = \mathbf{K}(\Lambda_a), \quad \Lambda_a = \omega_a^2 \tag{19}$$

and, by Leung's theorem [16],

$$\mathbf{M}_a = -\frac{\mathrm{d}\mathbf{K}_a}{\mathrm{d}\Lambda} = -\frac{1}{2\omega_a}\frac{\mathrm{d}\mathbf{K}_a}{\mathrm{d}\omega}. \tag{20}$$

As in Section 4, the force vector $[\mathbf{M}_a\mathbf{D}]$ is assembled without the need to form $\mathbf{M}_a$ explicitly, and the same is true for the other force vectors shown in square brackets [] in Sections 5 and 6.

The eigenvalue problem may be solved for μ^* by modifying the inverse iteration procedure of Eqs. (14)–(16), so that

$$\bar{\mathbf{D}}^{(k+1)} = \mathbf{K}_a^{-1}\left[\mathbf{M}_a\mathbf{D}^{(k)}\right], \tag{21}$$

$$\mu^{*(k+1)} = \frac{\left(\bar{\mathbf{D}}^{(k+1)}\right)^{\mathrm{T}}\left[\mathbf{M}_a\mathbf{D}^{(k)}\right]}{\left(\bar{\mathbf{D}}^{(k+1)}\right)^{\mathrm{T}}\left[\mathbf{M}_a\bar{\mathbf{D}}^{(k+1)}\right]}, \tag{22}$$

and the natural frequency ω_g is estimated by

$$\omega_\mu^* = \sqrt{\Lambda_a + \mu^*}. \tag{23}$$

Comparison of Eqs. (18)–(20) and (23) with Eqs. (11)–(13) shows that

$$\omega_\mu = \frac{\omega_a^2 + \omega_\mu^{*2}}{2\omega_a}, \tag{24}$$

so that the estimates ω_μ and ω_μ^* differ by

$$(\omega_\mu - \omega_\mu^*) = \frac{(\omega_a - \omega_\mu^*)^2}{2\omega_a}. \tag{25}$$

The $\underline{\mathbf{K}}(\Lambda)$ formulation is exactly equivalent to using exact shape functions in the usual FEM approach. Because the FEM solution is known to yield an upper bound on the required natural frequency, it follows from Eq. (25) that

$$\omega_\mu > \omega_\mu^* > \omega_g. \tag{26}$$

Thus, for sufficiently close lower and upper bounds (ω_ℓ, ω_u), the $\mathbf{K}(\Lambda)$ formulation is expected to be superior to the $\mathbf{K}(\omega)$ formulation.

Two simple examples were used to compare the estimates ω_μ and ω_μ^* obtained, respectively, from the $\mathbf{K}(\omega)$ and $\mathbf{K}(\Lambda)$ formulations. The examples are a cantilever and a cross-shaped plane frame consisting of four identical members, two being vertical and two horizontal, which are

Table 1
Accuracy of ω_μ and ω_μ^* for the first two axial natural frequencies of a cantilever and for the fundamental flexural natural frequency of a cross-shaped frame

Structure	Cantilever		Cross
i	1	2	1
ω_i (rad/s)	1.5707963	4.7123890	15.418206
ω_a/ω_i	1.0693875	1.0085152	1.0012210
ω_μ/ω_i	1.0085152	1.0000803	1.0000026
ω_μ^*/ω_i	1.0066765	1.0000447	1.0000018

rigidly connected together at their common node and built in at the other ends. For simplicity, the members for both examples have length and mass per unit length equal to unity. Additionally, $EA = 1$ for the cantilever, for which the natural frequencies ω_1 and ω_2 are the first two axial ones; and $EI = 1$ for the cross-shaped frame, for which $EA = 10^6$ was used to simulate inextensible members and the fundamental (flexural) natural frequency ω_1 was found.

The results in Table 1 confirm the predictions of Eq. (26) that using $\mathbf{K}(\Lambda)$ instead of $\mathbf{K}(\omega)$ gives significantly closer approximations to the exact natural frequency. Because the method is recursive, this benefit will accumulate as successive inverse iteration problems are solved, where each problem more closely represents the true transcendental one because its formulation uses the results from the previous problem. For this reason, use of the $\mathbf{K}(\Lambda)$ formulation will be assumed for the remainder of this paper.

6. Recursive Newton method with substructures

The normal form of substructuring implies the partitioning of $\mathbf{K}_a$ shown in Eq. (5) which, with Eq. (7), defines the subscripts and superscripts used in this section for this and the analogous partitioning of $\mathbf{M}_a$. As in Section 4, the subscript a denotes quantities evaluated at $\omega = \omega_a$. The substructuring leads to the final structure matrix $(\mathbf{K}_{pT}^*)_a$ of Eq. (7), which then replaces $\mathbf{K}_a$ in Eq. (11), so that $\mathbf{M}_a$ is replaced analogously by $(\mathbf{M}_{pT}^*)_a$, which must be found by differencing. However Eq. (8) shows that $(\mathbf{K}_{pT}^*)_a$, and hence $(\mathbf{M}_{pT}^*)_a$, will be ill conditioned whenever any $\mathbf{K}_{iis}$ is close to being singular, i.e. whenever the required natural frequency of the structure is too close to a natural frequency of a substructure when the nodes at which it is connected to its parent structure are clamped. Therefore traditional exact substructuring is unreliable, and hence not viable, when used with the recursive Newton method [14], or indeed with the second-order method either [13]. The remainder of this section overcomes this deficiency by using substructure matrices in a manner which is analogous to working with Eq. (5), i.e. without substructuring, during inverse iteration in order to improve the numerical conditioning.

When substructures $S_1, S_2, \ldots, S_{n_s}$ are present, the new method solves Eq. (18) but with its $\mathbf{K}_a$ replaced by the square matrix on the left hand side of Eq. (5) and $\mathbf{M}_a$ replaced by an analogously partitioned matrix. Thus the inverse iteration procedure of Eq. (21) is implemented as follows.

Force vectors

$$\mathbf{X}_{is} = \left[(\mathbf{M}_{iis})_a \mathbf{D}_{is}^{(k)}\right] + \left[(\tilde{\mathbf{M}}_{ics})_a \mathbf{D}_p^{(k)}\right] \quad (s = 1, 2, \ldots, n_s) \tag{27}$$

and

$$\mathbf{X}_p = \sum_{s=1}^{n_s} \left[\left(\tilde{\mathbf{M}}_{ics}\right)_a^{\mathrm{T}} \mathbf{D}_{is}^{(k)}\right] + [(\mathbf{M}_{pT})_a \mathbf{D}_p^{(k)}] \tag{28}$$

are formed for the substructure and parent structure, respectively, by summing contributions from individual members. Eq. (18) now has the form of Eq. (5) and is solved, after transformation to the form of Eq. (7), as follows.

First the displacements of the parent structure are found by

$$\bar{\mathbf{D}}_p^{(k+1)} = (\mathbf{K}_{pT}^*)_a^{-1} \mathbf{X}_p^*, \tag{29}$$

and then the internal displacements $\bar{\mathbf{D}}_{is}^{(k+1)}$ of each substructure are found efficiently by back-substitution into

$$(\mathbf{K}_{iis}^{\Delta})_a \bar{\mathbf{D}}_{is}^{(k+1)} = \mathbf{X}_{is}^* - (\tilde{\mathbf{K}}_{ics}^*)_a \bar{\mathbf{D}}_p^{(k+1)} \quad (s = 1, 2, \ldots, n_s). \tag{30}$$

The partitioned form of Eq. (5) permits the Rayleigh quotient of Eq. (22) to be calculated, by efficiently separating the contributions from each of the substructures and the parent structure, as

$$\mu^{*(k+1)} = \frac{\sum_{s=1}^{n_s} \bar{\mathbf{D}}_s^{(k+1)^{\mathrm{T}}} [(\mathbf{M}_s)_a \mathbf{D}_s^{(k)}] + \bar{\mathbf{D}}_p^{(k+1)^{\mathrm{T}}} [(\mathbf{M}_p)_a \mathbf{D}_p^{(k)}]}{\sum_{s=1}^{n_s} \bar{\mathbf{D}}_s^{(k+1)^{\mathrm{T}}} [(\mathbf{M}_s)_a \bar{\mathbf{D}}_s^{(k+1)}] + \bar{\mathbf{D}}_p^{(k+1)^{\mathrm{T}}} [(\mathbf{M}_p)_a \bar{\mathbf{D}}_p^{(k+1)}]}, \tag{31}$$

where

$$\bar{\mathbf{D}}_s^{(k+1)} = \begin{bmatrix} \bar{\mathbf{D}}_{is} \\ \bar{\mathbf{D}}_p \end{bmatrix}^{(k+1)}, \quad \mathbf{D}_s^{(k)} = \begin{bmatrix} \mathbf{D}_{is} \\ \mathbf{D}_p \end{bmatrix}^{(k)}, \quad (\mathbf{M}_s)_a = \begin{bmatrix} \mathbf{M}_{iis} & \tilde{\mathbf{M}}_{ics} \\ \tilde{\mathbf{M}}_{ics}^T & \tilde{\mathbf{M}}_{ccs} \end{bmatrix}_a. \tag{32}$$

Since the inverse iteration involves triangulating $\mathbf{K}(\Lambda_a)$, $J(\omega_a)$ can easily be found, so that it is immediately known from the W–W algorithm whether ω_a is an upper or lower bound on ω_g. Thus the frequency interval (ω_ℓ, ω_u) can be updated for use in subsequent convergence tests. To prevent an excessive number of iterations being required when convergence is in one direction, a minimum step size is enforced, as in Ref. [14].

This section has illustrated the use of exact substructuring in an exact $\mathbf{K}(\Lambda)$ formulation of the recursive Newton method. Such substructuring tools could similarly be implemented in any inverse iteration method, e.g. in conjunction with: exact or linear approaches; $\mathbf{K}(\Lambda)$ or $\mathbf{K}(\omega)$ formulations; and recursive or second-order convergence.

7. Examples

This section contains numerical examples to illustrate the substructuring theory. The structures used are all rigidly jointed plane frames. Also, the term mode is interpreted to mean the amplitudes of vibration at the nodes, i.e. **D** of Eq. (1), although members also vibrate between nodes and often have their largest displacements there. Therefore all modes referred to are normalised such that their largest element, i.e. the largest element of **D**, is unity. All the results were obtained using double precision arithmetic on a computer giving at least 14 significant figures of accuracy. Where appropriate, natural frequencies and modes are printed to two figures more than the specified solution tolerance, in order to demonstrate convergence. Relative differences are given to three significant figures, except where this would imply precision beyond the solution tolerance.

The first example is used to validate the method and to demonstrate its efficiency for general substructures. Next, the second example illustrates the use of substructuring to insert interior nodes into members. Then Examples 3 and 4 are ones which were specially designed to explore the possibility of ill conditioning for some special cases. They are relevant to substructuring in general, but are specifically for interior nodes substructuring. Such ill conditioning is known [14] to be avoided by numbering the interior nodes last and including them when assembling the dynamic stiffness matrix of the structure, which is thus expanded by the addition of extra rows at its bottom and extra columns at its right hand boundary. The examples investigate whether it is also avoided by numbering the interior nodes first, as implied by the substructuring methods of this paper.

Example 1. This example is used to validate the general substructuring method. The fairly large frame shown in Fig. 2(a) has 153 nodes (the last three of which are fixed) and 330 members. All horizontal members are 1.50 m in length and all vertical members are 1.00 m in length. The properties for the members are $EA = 9.0 \times 10^8$ N, $EI = 5.0 \times 10^6$ N m^2 and mass per unit length = 35 kg/m. The tolerance used for the solution was $\varepsilon = 10^{-10}$.

In the absence of any known exact solution for this structure, the first five natural frequencies ($\omega_1 - \omega_5$) and the corresponding modes of vibration for the full structure without using substructuring were first computed to be used as a datum. The structure was then modelled as a parent structure S_p and the two substructures S_1 and S_2 each repeated five times, as shown in Fig. 2(b).

The computed results are shown in Table 2. These results show that the natural frequencies and modes obtained using substructuring fully agreed with the datum ones obtained by modelling the full frame. The mode shapes are not shown in detail, but the first, second, fourth and fifth were sway modes and so were anti-symmetric about the vertical axis of symmetry of the frame, while the third mode was a symmetric one in which the 'trunk' extended and each 'branch' flexed upwards.

Further investigations to assess the reduction in solution time were carried out with and without substructuring for three cases:

(a) First five natural frequencies ($\omega_1 - \omega_5$) and modes, using the general substructuring of Fig. 2(b).
(b) Five close natural frequencies ($\omega_{109} - \omega_{113}$) and their modes, again using the general substructuring of Fig. 2(b).

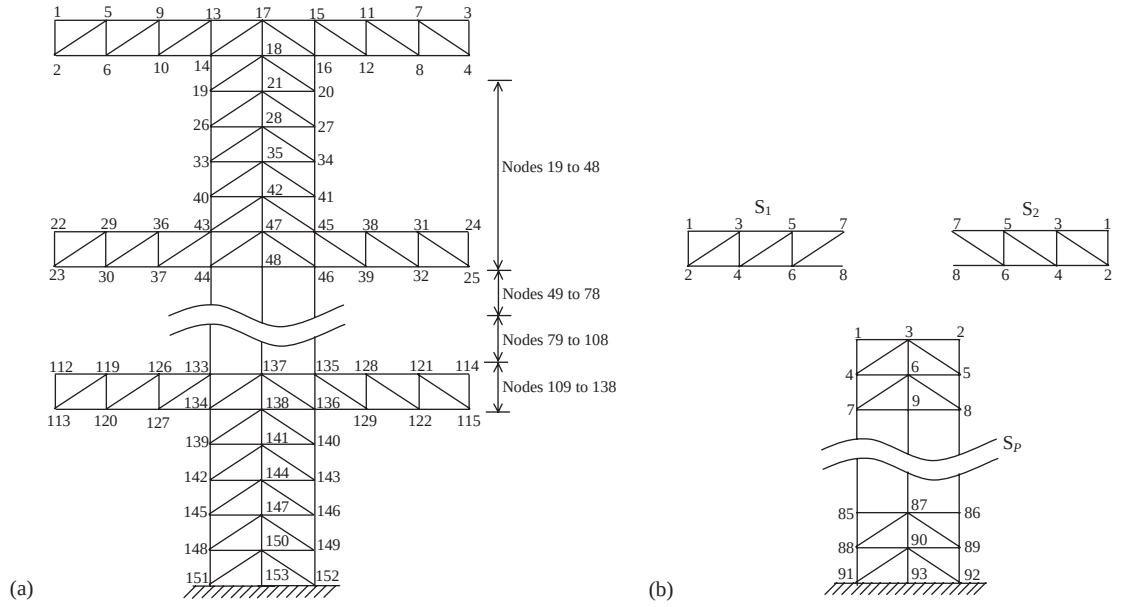

Fig. 2. Frame of Example 1: (a) original frame; (b) substructuring as parent structure S_p and five substructures of each of types S_1 and S_2.

Table 2
Accuracy of natural frequencies and modes obtained by substructuring for Example 1, to which Fig. 2 relates

Natural frequency no., i	Datum natural frequency ω_i, with no substructuring (rad/s)	Relative difference between substructuring and datum natural frequencies	Maximum absolute difference between substructuring and datum mode elements
1	9.972655692	-3×10^{-12}	5×10^{-13}
2	51.21750639	4×10^{-13}	5×10^{-13}
3	106.7960373	-3×10^{-14}	7×10^{-13}
4	108.2997767	6×10^{-14}	6×10^{-13}
5	142.3326898	-2×10^{-14}	5×10^{-13}

(c) One natural frequency (ω_{170}) and mode where an interior node is required in every diagonal member.

Solution times and iteration counts for the various stages of the solution are given in Table 3, together with percentage reductions in the total solution time obtained by using substructuring. It is seen that modest time savings result from the use of general substructuring in cases (a) and (b), largely due to improved efficiency in the triangulation of **K** during the initial separation of eigenvalues. In case (c) there is also a substantial time saving in the inverse iteration phase when the interior nodes are handled efficiently by substructuring instead of being numbered last.

Table 3
Efficiency of substructuring for three cases of Example 1, to which Fig. 2 relates

Solution type	Case Natural frequencies	(a) $\omega_1-\omega_5$	(b) $\omega_{109}-\omega_{113}$	(c) ω_{170}
Datum	Time for initial eigenvalue separation (s)	0.22	0.32	0.15
No substructures used	Time for inverse iterations (s)	1.10	1.09	7.24
For case (c) interior nodes are used and numbered last	Total time (s)	1.32	1.41	7.39
	No. of iterations for initial eigenvalue separation	13	19	8
	No. of Newton iterations	20	22	6
	No. of inverse iterations	65	58	39
Substructures used	Time for initial eigenvalue separation (s)	0.13	0.19	0.12
For cases (a) and (b) the substructures are those of Fig. 2(b)	Time for inverse iterations (s)	0.96	1.04	2.16
	Total time (s)	1.09	1.23	2.28
For case (c), substructures are used to handle the interior nodes	No. of iterations for initial eigenvalue separation	13	19	8
	No. of Newton iterations	18	22	6
	No. of inverse iterations	61	60	39
	Reduction of total time (%)	17.4	12.8	69.1

Example 2. This example is used to validate the interior nodes substructuring. Fig. 3(a) shows a frame with three nodes and two members. The length L of each member is 1 m. The member properties are $EA = 1.0 \times 10^6$ N, $EI = 1.0\,\mathrm{N\,m^2}$ and mass per unit length = 1.0 kg/m. The tolerance used was $\varepsilon = 10^{-10}$.

Because the value of EA is artificially high and vertical and horizontal deflections of node 1 (see Fig. 3(a)) were artificially constrained to be zero, the second natural frequency of the frame coincides with the lowest fixed end frequency of each member, at 22.3732854481 rad/s. Therefore an interior node must be added in each member, in order to remove poles of elements of $\mathbf{K}(\Lambda)$ by shifting the member fixed end frequency.

The new frame to be analysed is given by Fig. 3(b). The interior nodes are inserted by analysing the frame as substructures S_1 and S_2 plus the parent structure S_p, as shown in Fig. 3(c). This effectively numbers the interior nodes first, as shown in Fig. 3(b). Note that S_1 and S_2 each consist of two members and three nodes, while the parent structure S_p has no members and three nodes.

Datum values of the second natural frequency and the corresponding mode of vibration of the frame were first computed from the whole frame numbered as shown in Fig. 3(d). Then the substructuring of Fig. 3(c) was used. The results are shown in Table 4, which shows them to be in full agreement.

Example 3. Example 3 covers vibration of the cross-shaped frame of Fig. 4. For simplicity all masses per unit length, flexural rigidities and lengths L were taken as unity, while the extensional rigidity EA was deliberately given the high value 10^6 to make the second and third natural frequencies close to the fourth one, making the problem of finding the fourth natural frequency

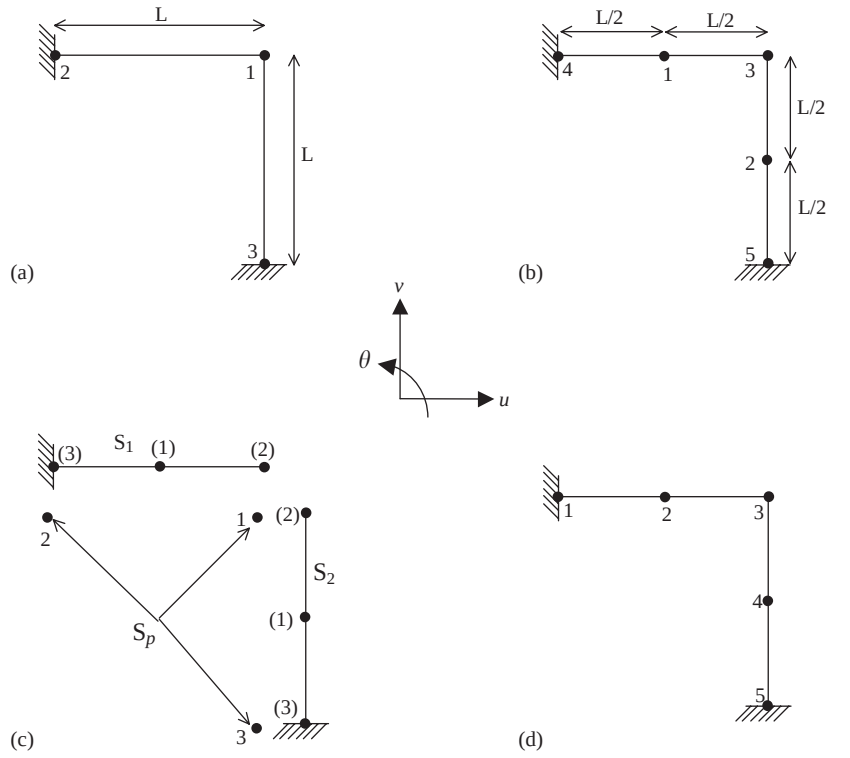

Fig. 3. Interior node substructuring for the frame of Example 2: (a) original frame, with three nodes; (b) addition of interior nodes; (c) parent structure S_p and substructures S_1 and S_2, with node numbers shown in brackets; (d) original frame with interior nodes but no substructuring.

Table 4
Second natural frequency (ω_2) and corresponding mode obtained for Example 2, to which Fig. 3 relates

ω_2 (rad/s)	No substructuring 22.3732854481			ω_2 (rad/s)	With substructuring 22.3732854481		
Nodes	Normalised mode			Nodes	Normalised mode		
	u	v	θ		u	v	θ
2	0.00000000000	1.00000000000	0.00000000000	S_1 node 1	0.00000000000	1.00000000000	0.00000000000
4	1.00000000000	0.00000000000	0.00000000000	S_2 node 1	1.00000000000	0.00000000000	0.00000000000
1, 3, 5	0.00000000000	0.00000000000	0.00000000000	S_p nodes 1–3	0.00000000000	0.00000000000	0.00000000000

and mode more demanding. The fourth natural frequency ω_4 for the frame is exactly equal to the fixed end frequency of its members, i.e. 22.373285448061 rad/s, while $\omega_2 = \omega_3 =$ 22.372318860018 rad/s.

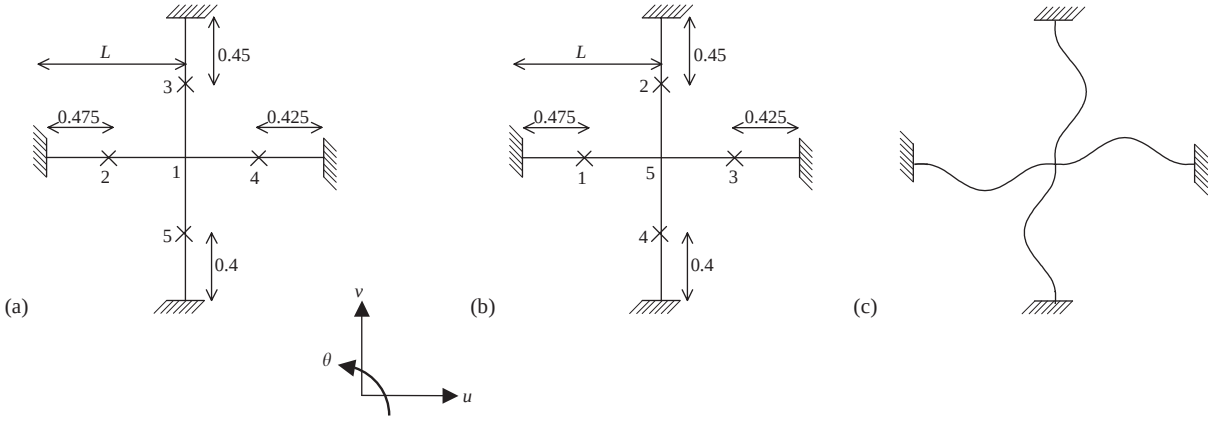

Fig. 4. Cross-shaped frame of Example 3: (a) interior nodes numbered last; (b) interior nodes numbered first; (c) correct mode for fourth natural frequency ω_4.

One interior node was inserted in each member slightly away from its centre and at the different positions shown in Fig. 4, to give both non-zero rotations and translations at these nodes. Two node numbering schemes were used; Fig. 4(a) shows the interior nodes numbered last and Fig. 4(b) shows these nodes numbered first, as would effectively be done by using substructuring. The mode is known to be that shown in Fig. 4(c), in which the four members are all vibrating as shown, with their fixed end mode and equal amplitudes. This mode gives force and moment equilibrium at the central node and so is clearly a possible mode of the frame. Therefore it is used as the comparator for the computed results which are shown in Table 5. They were obtained using a tolerance of $\varepsilon = 10^{-12}$ and can be seen to be in good agreement, with the maximum difference in any element of the mode being about 1.2×10^{-12}. Additional checks, involving subdivision of a single member with fixed ends, showed that the mode was indeed that of Fig. 4(c) to an accuracy of approximately 7.6×10^{-13}.

Example 4. Example 4 covers vibration of the quadrilateral frame shown in Fig. 5. The member properties are the same as those for Example 3 and the dimensions are given via the node coordinates shown in Fig. 5. Member 2–3 has a length of unity and a fixed end frequency $\omega_{Fm} = 22.372854481$ rad/s. The y coordinate h for node 4 was chosen to make ω_{Fm} match ω_6, the sixth natural frequency of the frame, to at least 12 significant figures, in order to test the performance of the substructuring method when a natural frequency of a substructure when its connection nodes to its parent structure are fixed coincides with the required natural frequency of the structure. This gave $h = 0.6337117216087$. The interior node divides member 2–3 in the ratio (0.45 : 0.55). The effect of the required frequency ω_6 becoming close to ω_{Fm} instead of coincident with it was investigated by slightly varying h, as shown in Tables 6 and 7. The results when the interior node was placed last are taken as a datum. Comparison with results obtained by bisection showed that these datum results had converged on ω_6 to 12 significant figures and they were therefore assumed to be free of ill conditioning. The normalised datum mode shape is listed in Table 8. In contrast to the modes found for Examples 2 and 3, this is not a mode for which the

Table 5
Fourth natural frequency (ω_4) and corresponding mode for the cross-shaped frame of Example 3, to which Fig. 4 relates

ω_4 (rad/s)	Interior nodes numbered last 22.373285448061			ω_4 (rad/s)	Interior nodes numbered first 22.373285448061		
Nodes	Normalised mode			Nodes	Normalised mode		
	u	v	θ		u	v	θ
1	0.000000000000	0.000000000000	0.000000000000	5	0.000000000000	0.000000000000	0.000000000000
2*	0.000000000000	−0.6102776993977	−0.2618886484244	1*	0.000000000000	−0.6102776993987	−0.2618886484249
3*	0.6005017678035	0.000000000000	0.5189912997972	2*	0.6005017678035	0.000000000000	0.5189912997973
4*	0.000000000000	0.5844075037588	−0.7665730088954	3*	0.000000000000	0.5844075037579	−0.7665730088942
5*	−0.5622911149409	0.000000000000	1.000000000000	4*	−0.5622911149409	0.000000000000	1.000000000000

The asterisks denote interior nodes.

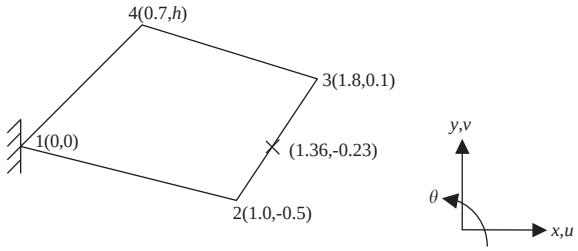

Fig. 5. Quadrilateral frame of Example 4, showing node numbers and coordinates. × denotes an interior node.

Table 6
Accuracy of the sixth natural frequency ω_6 and of the corresponding mode for the quadrilateral frame of Example 4, to which Fig. 5 relates

	No interior node			Interior node numbered first		
h	Relative difference between substructuring and datum natural frequencies	Maximum absolute difference between substructuring and datum mode elements	Number of inverse iterations	Relative difference between substructuring and datum natural frequencies	Maximum absolute difference between substructuring and datum mode elements	Number of inverse iterations
0.6337	-1.81×10^{-9}	1.93×10^{-8}	24	-4×10^{-14}	4×10^{-13}	9
0.6337038	-7.50×10^{-10}	2.85×10^{-8}	12	-4×10^{-13}	3×10^{-12}	11
0.6337064	-5.92×10^{-9}	7.72×10^{-8}	42	3×10^{-13}	6×10^{-12}	10
0.6337082	1.95×10^{-8}	1.09×10^{-7}	67	-2×10^{-13}	2×10^{-12}	10
0.6337093	2.32×10^{-8}	1.62×10^{-7}	37*	-8×10^{-14}	1.0×10^{-11}	12
0.6337101	3.80×10^{-8}	4.43×10^{-7}	17	7×10^{-13}	5×10^{-12}	12
0.6337106	3.64×10^{-8}	1.08×10^{-6}	101	7×10^{-13}	7×10^{-12}	10
0.6337110	7.83×10^{-8}	5.77×10^{-6}	463*	2×10^{-12}	6×10^{-12}	34
0.6337112	2.01×10^{-7}	8.17×10^{-6}	409*	-5×10^{-12}	1.9×10^{-11}	18
0.6337114	5.90×10^{-8}	2.19×10^{-4}	603*	5×10^{-12}	3.6×10^{-11}	28
0.6337115	-4.15×10^{-8}	2.21×10^{-3}	558*	-2×10^{-12}	9.1×10^{-11}	26

The asterisks indicate that the inverse iteration procedure failed to converge on at least one Newton iteration.

ends of member 2–3 are effectively fixed, the proximity of ω_6 and ω_{Fm} being merely a numerical coincidence.

Table 6 shows that, if the interior node is omitted, ill conditioning causes a loss of accuracy in both the eigenvalue and the mode as ω_6 approaches ω_{Fm}. Eventually the method fails as the inverse iteration procedure either converges on frequencies outside the interval (ω_ℓ, ω_u) or fails to converge at all. Table 7 shows that, if the interior node is included but numbered first (as is implied by the substructuring method of this paper), there is an acceptably small loss of accuracy, i.e. it is unlikely to cause concern until the required natural frequency is pathologically close to the member fixed end frequency.

Table 7
Accuracy of the sixth natural frequency ω_6 and of the corresponding mode for the quadrilateral frame of Example 4, to which Fig. 5 relates, with the interior node numbered first

h	Relative difference between substructuring and datum natural frequencies	Maximum absolute difference between substructuring and datum mode elements	Number of inverse iterations
0.6337	-4×10^{-14}	4×10^{-13}	9
0.6337115	-2×10^{-12}	9.1×10^{-11}	26
0.63371172	2.34×10^{-10}	3.13×10^{-9}	306*
0.6337117216	5.74×10^{-10}	5.55×10^{-8}	500*
0.6337117216087	1.15×10^{-10}	2.07×10^{-7}	163*

The asterisks indicate that the inverse iteration procedure failed to converge on at least one Newton iteration.

Table 8
Normalised datum mode corresponding to the sixth natural frequency ω_6 for the quadrilateral frame of Example 4, to which Fig. 5 relates, with the interior node numbered last

Nodes	Normalised mode		
	u	v	θ
1	0.000000000000	0.000000000000	0.000000000000
2	0.014619892935	0.029242904807	0.065226160330
3	−0.036140133916	0.096909238138	0.594243464856
4	−0.054130234999	0.059761731782	1.000000000000
5	0.018952777344	0.023461923532	−0.038732753519

8. Conclusions

The exact substructuring approach has been successfully extended to the guided recursive Newton method for solving transcendental eigenproblems, the principal objective being to calculate modes accurately and efficiently. Performing inverse iteration on the degrees of freedom of the parent structure alone is prone to numerical ill conditioning whenever a required eigenvalue lies close to an eigenvalue of any of the substructures when clamped at its attachment nodes. Therefore the inverse iteration algorithm presented includes all of the degrees of freedom at the internal nodes of the substructures. This retains the established accuracy of the method when substructures are not used, while improving the computational efficiency.

The substructuring method has been used to model the interior nodes which are inserted to remove member fixed end eigenvalues whenever they are dangerously close to a sought eigenvalue of the structure. Previously such nodes were numbered after the other nodes of the structure, which adversely affects the banded nature of the dynamic stiffness matrix and so often greatly increases the time taken by the inverse iteration. Treating the member and its interior node as a simple substructure effectively numbers the interior nodes before the other nodes and so gives a

much faster solution, both because it leaves the bandwidth of the stiffness matrix of the parent structure unaltered and also because savings result when some of the substructures are identical.

In the transcendental eigenproblem of vibration, the elements of the dynamic stiffness matrix contain trigonometric and hyperbolic functions of frequency ω. However it has been shown that it is preferable to use ω^2 rather than ω as the eigenparameter when locally approximating the transcendental eigenproblem as a generalised linear eigenproblem. This is true because: polynomial expansions of the member stiffnesses contain only even functions of ω; it follows from an analogy with a hypothetical FEM model with an infinite number of degrees of freedom; and it has been shown, both theoretically and numerically, that using ω^2 rather than ω gives significantly closer approximations to the exact eigenvalue at a typical step of the inverse iteration algorithm.

Numerical results have validated the use of substructuring to analyse a moderately large structure, giving no loss of accuracy in the eigenvalues or modes while making significant reductions in the overall solution times, particularly when members with interior nodes are modelled as substructures.

The use of substructures to model interior nodes has also been explored numerically on a number of simple examples which were designed to trigger numerical ill conditioning because of the proximity of structural eigenvalues to member fixed end eigenvalues. Such ill conditioning was not completely removed by modelling the interior nodes within substructures, but the results show that its effects are only likely to be significant when the member fixed end eigenvalues are pathologically close to the structural eigenvalue being sought. In such circumstances, accuracy could be improved by using the previous method of numbering the interior nodes after the other nodes, without using substructuring.

The exact substructuring methods presented have been illustrated by their implementation in one particular inverse iteration scheme, but they could equally well be applied to other forms of inverse iteration. They are also applicable to various other areas of structural analysis to which the W–W algorithm has successfully been applied (e.g. wave propagation), as well as to problems in other disciplines, including fluid vibrating in pipes, heat and mass diffusion, and mathematical problems involving Sturm–Liouville equations.

Acknowledgements

The authors gratefully acknowledge financial support from the Engineering and Physical Sciences Research Council (grant number GR/R05406/01), the National Natural Science Foundation of China, City University of Hong Kong and the Cardiff Advanced Chinese Engineering Centre. The third author holds a chair at Cardiff University, to which he will return upon completion of his present appointment at City University of Hong Kong.

References

[1] F.W. Williams, W.H. Wittrick, An automatic computational procedure for calculating natural frequencies of skeletal structures, *International Journal of Mechanical Sciences* 12 (1970) 781–791.

[2] W.H. Wittrick, F.W. Williams, A general algorithm for computing natural frequencies of elastic structures, *Quarterly Journal of Mechanics and Applied Mathematics* 24 (1971) 263–284.
[3] W.H. Wittrick, F.W. Williams, An algorithm for computing critical buckling loads of elastic structures, *Journal of Structural Mechanics* 1 (1973) 497–518.
[4] W.H. Wittrick, F.W. Williams, Buckling and vibration of anisotropic or isotropic plate assemblies under combined loadings, *International Journal of Mechanical Sciences* 16 (1974) 209–239.
[5] F.W. Williams, Natural frequencies of repetitive structures, *Quarterly Journal of Mechanics and Applied Mathematics* 24 (1971) 285–310.
[6] F.W. Williams, D. Kennedy, Reliable use of determinants to solve non-linear structural eigenvalue problems efficiently, *International Journal for Numerical Methods in Engineering* 26 (1988) 1825–1841.
[7] D. Kennedy, F.W. Williams, More efficient use of determinants to solve transcendental structural eigenvalue problems reliably, *Computers and Structures* 41 (1991) 973–979.
[8] F.W. Williams, D. Kennedy, M.S. Djoudi, The member stiffness determinant and its uses for the transcendental eigenproblems of structural engineering and other disciplines, *Proceedings of The Royal Society: Mathematical, Physical and Engineering Sciences* 459 (2003) 1001–1019.
[9] F.W. Williams, D. Kennedy, M.S. Djoudi, Exact determinant for infinite order FEM representation of a Timoshenko beam-column via improved transcendental member stiffness matrices, *International Journal for Numerical Methods in Engineering* 59 (2004) 1355–1371.
[10] C.T. Hopper, F.W. Williams, Mode finding in nonlinear structural eigenvalue calculations, *Journal of Structural Mechanics* 5 (1977) 255–278.
[11] H.R. Ronagh, R. Lawther, F.W. Williams, Calculation of eigenvectors with uniform accuracy, *Journal of Engineering Mechanics* 121 (1995) 948–955.
[12] S. Yuan, K. Ye, F.W. Williams, Towards exact computation of vibration modes in dynamic stiffness methods, *Proceedings of the Fifth International Symposium on Structural Engineering for Young Experts*, Shenyang, China, 1998, pp. 11–19.
[13] S. Yuan, K. Ye, F.W. Williams, Second order mode-finding method in dynamic stiffness matrix methods, *Journal of Sound and Vibration* 269 (2004) 689–708.
[14] S. Yuan, K. Ye, F.W. Williams, D. Kennedy, Recursive second order convergence method for natural frequencies and modes when using dynamic stiffness matrices, *International Journal for Numerical Methods in Engineering* 56 (2003) 1795–1814.
[15] A. Simpson, On the solution of $\mathbf{S}(\omega) = \mathbf{0}$ by a Newtonian procedure, *Journal of Sound and Vibration* 97 (1984) 153–164.
[16] A.Y.T. Leung, *Dynamic Stiffness and Substructures*, Springer, London, 1993.
[17] A. Frid, Fluid vibration in piping systems: a structural mechanics approach. I. Theory, *Journal of Sound and Vibration* 133 (1989) 423–438.
[18] M.D. Mikhailov, M.N. Ozisik, N.L. Vulchanov, Diffusion in composite layers with automatic solution of the eigenvalue problem, *International Journal of Heat and Mass Transfer* 26 (1983) 1131–1141.
[19] M.D. Mikhailov, M.N. Ozisik, *Unified Analysis and Solutions of Heat and Mass Diffusion*, Wiley, New York, 1984.
[20] M.D. Mikhailov, N.L. Vulchanov, Computational procedure for Sturm–Liouville problems, *Journal of Computational Physics* 50 (1983) 323–336.
[21] J.H. Wilkinson, *The Algebraic Eigenvalue Problem*, Clarendon, Oxford, 1965.
[22] A. Jennings, *Matrix Computation for Engineers and Scientists*, Wiley, London, 1977.
[23] A. Simpson, B. Tabarrok, On Kron's eigenvalue procedure and related methods of frequency analysis, *Quarterly Journal of Mechanics and Applied Mathematics* 21 (1968) 1–39.
[24] W.H. Wittrick, F.W. Williams, New procedures for structural eigenvalue calculations, *Proceedings of the Fourth Australasian Conference on the Mechanics of Structures and Materials*, Brisbane, Australia, 1973, pp. 299–308.